Allosteric Interaction of Minor Groove Binding Ligands with UL9−DNA Complexes[†]

Yan Kwok,[‡] Wentao Zhang,*[,‡] Gary P. Schroth,[§] Cynthia H. Liang,[||] Nancy Alexi, and Thomas W. Bruice[⊥]

Genelabs Technologies, Inc., 505 Penobscot Drive, Redwood City, California 94063

Received May 14, 2001; Revised Manuscript Received August 13, 2001

ABSTRACT: The herpes simplex virus type 1 origin binding protein (UL9) is a sequence-specific DNA binding protein. Several studies have demonstrated that UL9 binds to the 11-base pair sequence 5′-CGTTCGCACTT-3′ primarily, or solely, through interaction with the major groove. Minor groove binding ligands, such as distamycin, netropsin, and GLX, an indole-linked dimer of netropsin, can effectively disrupt the UL9−DNA complex only when their DNA binding sites are coincident with the right side of the DNA binding site of the protein and overlap with the protein binding site by two (TT) base pairs. These results suggest that the right side of the UL9−DNA complex has a unique structure that is sensitive to minor groove ligand binding. In addition, a biphasic displacement curve was observed with GLX, which suggests two modes of ligand binding which have different effects on UL9−DNA complexes. Using a fluorescence-based hybridization stabilization assay, we determined that GLX can bind to its binding site as an overlapping dimer (i.e., 2:1 stoichiometry). Footprinting of UL9−DNA complexes with the minor groove directed chemical nuclease 1,10-phenanthroline copper confirms that the DNA conformation at the position of the right-side ligand binding site of GLX is altered and has a widened minor groove. In contrast, it is well established that at 1:1 stoichiometries, AT sequence specific ligands, such as netropsin, distamycin, and GLX, prefer uniform, narrow minor grooves. The opposing conformational requirements of UL9 and lower concentrations of GLX at the ligand binding A-tract overlapping the right side of the protein binding site indicate that allosteric inhibition, rather than direct steric competition, contributes to ligand-induced protein displacement. At higher GLX concentrations, giving 2:1 binding in a widened minor groove, co-binding with UL9 is allowed. A model is presented that is consistent with these observations, and implications for targeted regulation of gene transcription are discussed.

Protein−DNA interactions are critical cellular events in regulating transcription and replication. Molecules that target specific sequences can disrupt these protein−DNA interactions, thereby modulating gene expression. Although most protein−DNA recognition processes occur in the DNA major groove, design of small molecules that specifically target the wide major groove has proven difficult (*1*). The effort in targeting the major groove has been limited largely to utilizing protein folding scaffolds, notably zinc fingers (*2*, *3*). Meanwhile, progress has been made recently in designing small organic molecules that target the minor groove, partially because it is easier to generate a large favorable contact interface in the deeper and narrower minor groove of canonical B-DNA (*1*, *4*, *5*). These small minor groove binding ligands (MGBLs)[1] have long been shown to interfere with the binding of proteins that recognize the minor groove of DNA. MGBLs such as distamycin, Hoechst 33258, and netropsin effectively inhibit the interaction of TATA box binding protein (TBP) with DNA, a protein that binds exclusively in the minor groove (*6*). Other MGBLs, such as hairpin-linked, synthetic polyamides, have been found to interfere with the transcription factor TFIIIA−DNA interaction (*7*). TFIIIA contains nine zinc fingers, among which zinc fingers 4 and 6 are essential for high-affinity DNA recognition in the minor groove (*8*−*10*). The interference is considered to be the consequence of steric competition of MGBLs with the proteins for common sites within the minor groove.

It can be more difficult for MGBLs to displace major groove binding proteins from critical regulatory elements due to lack of direct steric interference. However, recent progress has shown MGBLs can compete off a number of major groove binding proteins, which represent the largest subset of regulatory transcription factors. One approach invokes chemical modification of the core MGBL. In one of the earliest studies of its kind, positively charged linear and

[†] This study was supported partially by DARPA UPC Program Grant N65236-98-1-5400.

* To whom correspondence should be addressed. Phone: (650) 369-9500. Fax: (650) 368-0709. E-mail: wentaoz@genelabs.com.

[‡] The first two authors contributed equally to this study.

[§] Present address: Applied Biosystems, 850 Lincoln Centre Dr., Foster City, CA 94404.

[||] Present address: MIT, Division of Bioengineering and Environmental Health, 77 Massachusetts Ave., 16-560, Cambridge, MA 02139.

[⊥] Present address: Biota Research Laboratories, 2232 Rutherford Rd., Carlsbad, CA 92008.

[1] Abbreviations: MGBL, minor groove binding ligand; TBP, TATA box binding protein; HSV-1, herpes simplex virus type 1; UL9, UL9 protein; ODNs, oligodeoxynucleotides; N, degenerate A, T, G, C base incorporation at a single sequence position of an ODN synthesis; MPA, mercaptopropionic acid; OP_2-Cu, 1,10-phenanthroline copper ion; EMSA, electrophoretic mobility shift assay; HSA, hybridization stabilization assay; T_m, duplex ODN thermal melting temperature; GLX, GL020924.

10.1021/bi0109865 CCC: $20.00
Published on Web 09/26/2001

branched polyamines were covalently conjugated to known MGBLs and were shown to be effective both for enhancing the affinity of interaction with DNA and for competing for binding with a protein that binds to both the major and minor grooves of DNA (*11*). In another example, synthetic polyamides have been shown to bind simultaneously with certain bZIP proteins that exclusively occupy the major groove (*12, 13*). However, when conjugated to a carboxy-terminal Arg-Pro-Arg tripeptide that delivers a positive patch to the DNA backbone, these synthetic polyamide−peptide conjugates were able to inhibit the binding of the GCN4 protein in the opposing major groove (*14*). These approaches involve the application of direct competition, in which the positive charges of the polyamines or tripeptide compete with the proteins for their contacts with the phosphates by neutralizing the negative charge of the DNA backbone and, in some cases, by also sterically blocking access to the major groove.

Another approach is to take advantage of DNA conformational changes upon binding of the proteins or MGBLs. For example, polyamide-bound DNA is resistant to the extensive bending and unwinding induced by TBP and LEF-1, another minor groove binding protein (*15*), thereby preventing them from binding to the protein recognition site adjacent to the polyamide's binding site (*16*). This allosteric effect also was seen with distamycin, which induces conformational changes of the DNA that preclude a homeodomain peptide from binding to the major groove (*17*). These studies have been performed with systems for which the protein−DNA complex crystal structures were known. It is of interest to explore the potential for disrupting major groove binding protein−DNA interactions with MGBLs that have not been chemically modified to interact with the backbone and/or major groove.

As a model system, we have studied the interactions of two natural product MGBLs and a novel designed MGBL with UL9−DNA complexes. The origins of DNA replication of herpes simplex virus type 1 (HSV-1) are recognized by the virus-encoded origin of replication binding protein, a product of the UL9 gene (*18, 19*). Binding of the origin of replication binding protein (UL9 protein) to specific elements within the HSV-1 replication origins is essential for the initiation of viral DNA replication. UL9 protein is a 94-kDa protein that possesses both sequence-specific DNA binding and ATP-dependent DNA helicase activities (*19*−*21*). The sequence-specific DNA binding activity of the UL9 protein resides in the C-terminal 317 amino acids (*22*). We have utilized the DNA binding C-terminal domain of UL9 in this study to dissect the DNA binding activity from the helicase activity. Several mutation and footprinting studies have mapped the DNA recognition site for the UL9 protein to an 11-bp sequence, 5′-CGTTCGCACTT-3′, within which the central 8-bp 5′-GTTCGCAC-3′ sequence contributes most of the specificity of complex formation (*23, 24*). It has been shown biochemically that the full-length UL9, as well as the C-terminal domain, binds to the recognition sequence as a homodimer (*25, 26*). Although there is no direct structural information for a UL9−DNA complex, cross-linking experiments suggested only one of the two monomers contacts DNA (*25*). Several studies have suggested that UL9 interacts with specific bases in the major groove of DNA. Methylation interference studies demonstrated that all five guanines within the central 5′-GTTCGCAC-3′ sequence are critical for UL9−DNA interaction, indicating that UL9 makes base-specific contacts with those guanines in the major groove (*27*). A recent study showed that methyl groups of the thymines in the major groove within the sequence 5′-GTTCGCAC-3′ were also essential for high-affinity binding of UL9, while changes in the minor groove had much less impact on protein binding (*28*). We have confirmed and extended these results with additional chemical interference agents (unpublished results). All of this evidence suggests that UL9 interacts with DNA primarily, or solely, through major groove contacts.

In the study reported here, we targeted the sequence positions overlapping and flanking the UL9 protein recognition site. In natural (wild-type) promoter sequences, the bases adjacent to critical regulatory elements are relatively nonconserved and, therefore, are attractive target sites of small molecules for gene-specific regulation (*29*). This strategy is preferable to targeting consensus transcription factor binding sequences only of critical regulatory elements—or directly or indirectly inhibiting the transcription factor itself—which would be expected to modulate expression of all genes regulated by that protein factor. Since MGBLs specific for AT sequences are the only ones readily available, we engineered AT sequence ligand binding sites at the flanking/overlapping sequence positions of UL9−DNA complexes. We demonstrate that MGBLs, distamycin and netropsin, are able to displace the major groove binding protein UL9 by binding to a site on the right side of the protein binding site that overlaps with the recognition sequence of the protein by two base pairs. Compound GLX, a rigid indole-linked dimer of netropsin-like dipyrrole polyamides, which recognizes longer AT sequences (*29, 30*), is 10−40-fold more potent at UL9 displacement at low ligand concentrations. However, GLX is much less effective at UL9 displacement at higher ligand concentrations, indicating two different binding modes may be involved. Binding stoichiometry studies show a 2:1 binding complex between GLX and DNA at higher ligand concentrations. Finally, 1,10-phenanthroline copper (OP_2-Cu) footprinting of UL9−DNA and GLX−DNA complexes indicates that allosteric inhibition, rather than direct competition, contributes to the displacement of UL9 protein by GLX at the lower concentrations. These results have immediate application to engineered gene switch constructs employing UL9 and GLX. They also provide evidence that similar allosteric mechanisms of gene expression regulation in natural systems may likely be used in the future concurrent with the sufficient availability of single base resolution sequence specific MGBLs.

EXPERIMENTAL PROCEDURES

Materials. Distamycin was purchased from Sigma, and netropsin was obtained from Boehringer Mannheim. GLX was synthesized by an alternative method to that published (*30*) as will be described in a separate report (Roberts et al., in preparation). The DNA binding domain of UL9 was expressed and purified as a GST fusion protein using the published method (*31*). 1,10-Phenanthroline monohydrate and 2,9-dimethyl-1,10-phenanthroline were from GFS Chemicals, Inc. Copper(II) sulfate anhydrous and 3-mercaptopropionic acid (MPA) were from Aldrich. Oligodeoxynucleotides (ODNs) were purchased from Sigma-Genosys (Woodland, TX). Electrophoretic reagents (acrylamide, *N*,*N*′-

methylenebisacrylamide, ammonium persulfate) were from Bio-Rad, and *N*,*N*,*N*′,*N*′-tetramethylethylenediamine (TEMED) was from Boehringer Mannheim. T4 polynucleotide kinase was purchased from New England Biolabs, and [γ-^{32}P]ATP was from Amersham.

Preparation and End-Labeling of Oligonucleotides. ODNs were purified by 12% denaturing polyacrylamide gel electrophoresis. The 5′ end-labeled single-stranded ODNs were obtained by incubating 10 μL of 1 μM samples of the ODNs with 5 units of T4 polynucleotide kinase and 5 μL of 3000 Ci/mmol [γ-^{32}P]ATP in a total final volume of 20 μL at 37 °C for 1 h. The labeled strand was then annealed with 1.3-fold of the sequence-complementary strand.

Electrophoretic Mobility Shift Assays (EMSAs). Binding was carried out in 20 μL of 20 mM HEPES, pH 7.5, 50 mM KCl, 0.1 mM EDTA, 5% glycerol, and 1 mM DTT. The binding interactions were initiated by incubating a 0.5 nM aliquot of end-labeled ODN DNA with 100 or 200 nM UL9 protein at ambient temperature for 20 min, followed by the addition of the ligand. The incubation continued for 1−2 h before being loaded onto an 8% native polyacrylamide gel (acrylamide:bisacrylamide ratio = 29:1).

OP_2-Cu Footprinting Experiments. The DNA binding was carried out in the same buffer and conditions, unless otherwise specified in the figure legends, as EMSAs except that 5% glycerol was omitted. The OP_2-Cu cleavage reaction was performed according to previously published procedures (*32*). Briefly, to a 20 μL binding reaction mixture containing labeled ODNs and protein were added 2 μL of a solution containing 9 mM $CuSO_4$, 40 mM 1,10-phenanthroline and 2 μL of 58 mM MPA. The reactions were allowed to proceed for 5 min at ambient temperature and were stopped by the addition of 2 μL of 28 mM 2,9-dimethyl-1,10-phenanthroline. The samples were loaded onto a 12% denaturing polyacrylamide gel and electrophoresed at 1600 V for 3 h.

Imaging and Quantification. The denaturing polyacrylamide gels were dried and exposed to phosphor screens (Molecular Dynamics). Imaging and quantification were performed using a PhosphorImager and ImageQuaNT software (Molecular Dynamics).

Binding Stoichiometry by Hybridization Stabilization Assay. The hybridization stabilization assay method will be described in detail elsewhere (Gonzalez et al., manuscript in preparation). The 11-bp ODN FQ11 (Figure 8) has a fluorescein fluorophore (F) at the 5′ end on one strand and a dabcyl quencher (Q) at the 3′ end on the complementary strand. These ODNs are designed with a T_m for the hybridized state slightly below ambient temperature so as to remain largely single-stranded in HEN buffer (10 mM HEPES, pH 7.2, 0.1 mM EDTA, and 10 mM NaCl). Since MGBLs bind to the minor groove of ds DNA, but not to ss DNA, addition of the drug induces duplex formation by stabilization of hybridization of the end-labeled ODNs. The hybridization of these complementary strands brings fluorescein and dabcyl in close proximity, thus quenching the fluorescence. Therefore, the HSA can be used to quantitatively measure DNA binding by MGBLs under isothermal conditions using fluorescence spectroscopy. Fluorescence was measured at an excitation wavelength of 485 nm and at an emission wavelength of 530 nm using a 96-well plate fluorometer (CytoFluor Series 4000, PerSeptives Biosystems).

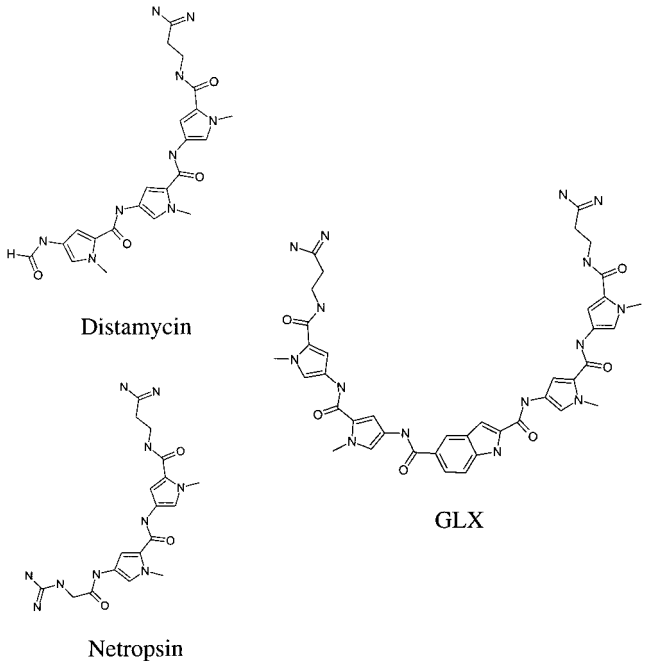

FIGURE 1: Structures of the compounds used in this study.

Determination of ligand binding stoichiometry was made using the hybridization stabilization assay applying the method of continuous variation (*33*), where the total concentration of GLX and DNA was kept constant at 0.5 μM. The molar fraction of the ligand was varied from 0 to 1. All experiments were performed in duplicate.

RESULTS

Distamycin and Netropsin Selectively Displace UL9 by Binding to the Right Side of the Protein Binding Site. The ability of distamycin (Figure 1), a MGBL (*34*), to displace the major groove binding protein UL9 was evaluated by EMSA. The ODNs were designed to contain the preferred ligand binding site, AATT (*35*, *36*), positioned at various "registers" on either the right or the left sides of the protein binding site. Figure 2A shows the sequences of the ODNs used for this study. The engineered ligand binding sites are highlighted in boldface type, while the UL9 binding sites are underlined. The "edges" of the UL9 binding site are represented by gaps in the sequences, and by slants in the ODN nomenclature. Each series starts with the AATT ligand binding site overlapping the UL9 binding site. The AATT site is then progressively moved further away from each edge of the protein binding site. Our selection study (unpublished data) and other published data (*24*) have demonstrated that the central 9-bp sequence 5′-GTTCGCACT-3′ within the UL9 binding site is highly conserved among all the UL9 binding sites, while the remaining base pairs at the edge of the protein binding site are less well conserved. Thus, the edge base pairs on either side of the UL9 binding site were changed either to accommodate and/or to fix the register of the ligand binding sites. None of these changes dramatically affected the binding of UL9 protein in the absence of the ligands, as shown in lane 2 in Figure 2B.

Distamycin was added to the UL9−DNA incubation mixture to determine whether this MGBL can disrupt a preformed UL9−DNA complex. The UL9−DNA complex

A.

Right side of UL9 test sites: **Name**

GTGCA CGTTCGCAC**TA ATT** CCG **TA/ATTCCG**
CACGT GCAAGCGTG**AT TAA** GGC

GTGCA CGTTCGCACTG **AATT** CCG **TG/AATTCC**
CACGT GCAAGCGTGAC **TTAA** GGC

GTGCA CGTTCGCACTG C**AATT** CCG **TG/CAATTC**
CACGT GCAAGCGTGAC G**TTAA** GGC

GTGCA CGTTCGCACTG GC**AATT** CCG **TG/GCAATT**
CACGT GCAAGCGTGAC CG**TTAA** GGC

Left side of UL9 test sites:

CGG **AAT TG**TTCGCACTG ACGTC **CGGAAT/TG**
GCC **TTA A**CAAGCGTGAC TGCAG

CGG **AATT** CGTTCGCACTG ACGTC **GGAATT/CG**
GCC **TTAA** GCAAGCGTGAC TGCAG

CGG **AATT**C CGTTCGCACTG ACGTC **GAATTC/CG**
GCC **TTAA**G GCAAGCGTGAC TGCAG

CGG **AATT**CC CGTTCGCACTG ACGTC **AATTCC/CG**
GCC **TTAA**GG GCAAGCGTGAC TGCAG

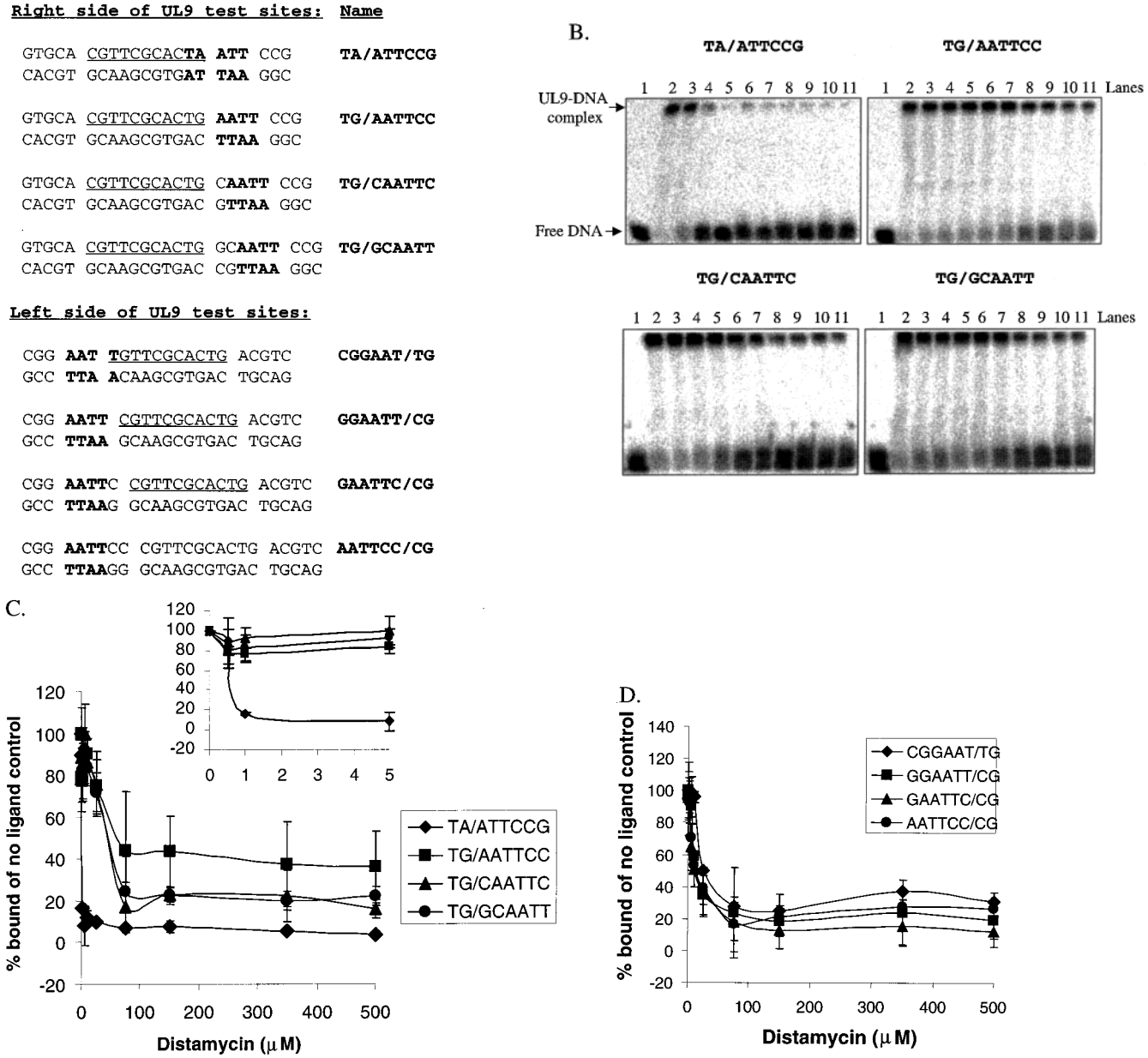

FIGURE 2: Effects of distamycin on UL9 displacement from specific positions on the left and right sides of the protein binding site. (A) ODNs used in this study. (B) Autoradiogram of an EMSA 8% native polyacrylamide gel showing the effect of the ligand on the UL9−DNA complex using the right-side ODNs. Lane 1 contains no protein. Lanes 2−11 contain 100 nM UL9, and 0, 0.5, 1, 5, 10, 25, 75, 150, 350, and 500 μM distamycin, respectively. (C) Quantitative analysis represented by a graph. The intensity of the bands indicated by arrows in (B) was quantitated using a PhosphorImager and analyzed using ImageQuaNT Software (Molecular Dynamics). "% UL9−DNA complex" was determined from the radioactivity contained in the volumes of bands of the UL9−DNA complex divided by the total radioactivity in each of the lanes. "% bound of no ligand control" was calculated from normalizing the "% UL9−DNA complex" by the no ligand control. The inset depicts an expanded scale for the low concentration range of ligand. (D) Effects of distamycin on the UL9−DNA complex using the left-side ODNs (gel not shown).

was separated from free DNA by an 8% native polyacrylamide gel. The fraction of DNA in the UL9−DNA complex was determined by phosphorimage analysis using the ImagQuaNT software from Molecular Dynamics. Figure 2B shows a representative EMSA in the presence of distamycin. The first ODN in the series, TA/ATTCCG, was designed with the ligand binding site of AATT overlapping the UL9 recognition sequence by one base pair on the right side of the UL9 protein. This was the only ODN in either series that showed strong ligand-induced displacement (Figure 2C,D). This ODN, TA/ATTCCG, actually has five A/Ts instead of four A/Ts, including the first T from the protein binding site. Therefore, the ligand binding site overlaps the protein binding site by two base pairs. With this ODN, the amount of distamycin required to disrupt 50% of the protein−DNA complex, compared to the no ligand controls (IC_{50}), is 0.5 μM. The other three right-side ODNs and all four of the left-side ODNs, including the first one that overlaps the UL9 binding site by 1 bp, had only modest activity, with IC_{50} values over 50 μM (Figure 2C,D). These results indicate that, for distamycin, there is a ligand binding register on the DNA which overlaps the right side of the

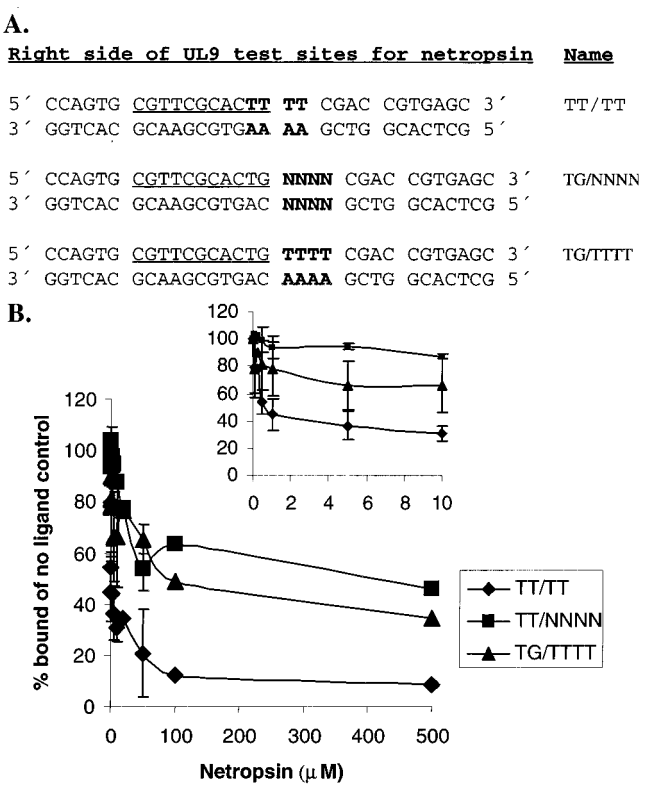

FIGURE 3: Effects of netropsin on UL9 displacement from the right side of the protein using the 5-bp binding sites. ODNs shown in Figure 2A also were used here. Quantitative analysis was the same as in Figure 2C, and the inset depicts an expanded scale for the low concentration range of ligand.

UL9 binding site, that must be occupied by ligand in order to observe strong ligand-induced displacement of protein.

Another MGBL, netropsin (Figure 1), also was examined for its ability to displace UL9−DNA complexes. While distamycin can discriminate among these right-side-tested ODNs with 100-fold differences in IC_{50} values, the discrimination was less significant in the case of netropsin (data not shown). Netropsin, which contains two pyrrole rings, has been shown to bind to DNA only as a monomer with a site size of four AT base pairs. In contrast, although it can bind to a minimal of four AT base pairs as a monomer (*34*, *36*−*38*), distamycin with three pyrrole rings forms a dimer upon binding to at least five consecutive AT-rich base pairs (*38*, *39*). ODN TA/ATTCCG, which contains 5 AT bp, is a little bigger than the minimum size AT site required for optimal binding and clamping of netropsin. Consequently, netropsin may slide out of the ligand binding register required for UL9 displacement. To test this hypothesis, ODNs were designed to have only four AT base pairs on the right side of the UL9 binding site (Figure 3A). The first ODN in the series, TT/TT, in which the 4-bp ligand binding site overlaps UL9 by two base pairs, shows much stronger displacement efficacy by netropsin, with an IC_{50} of 0.8 μM (Figure 3B). The IC_{50} of netropsin with two other ODNs, TG/TTTT and TG/NNNN (a randomized sequence control ODN), was significantly increased to around 50−100 μM. Similarly to distamycin, netropsin could not effectively displace UL9 from the left side of the protein (data not shown). These results again support the conclusion that the major groove binding protein UL9 can be displaced by MGBLs with the most preferred register of high-affinity ligand binding sites.

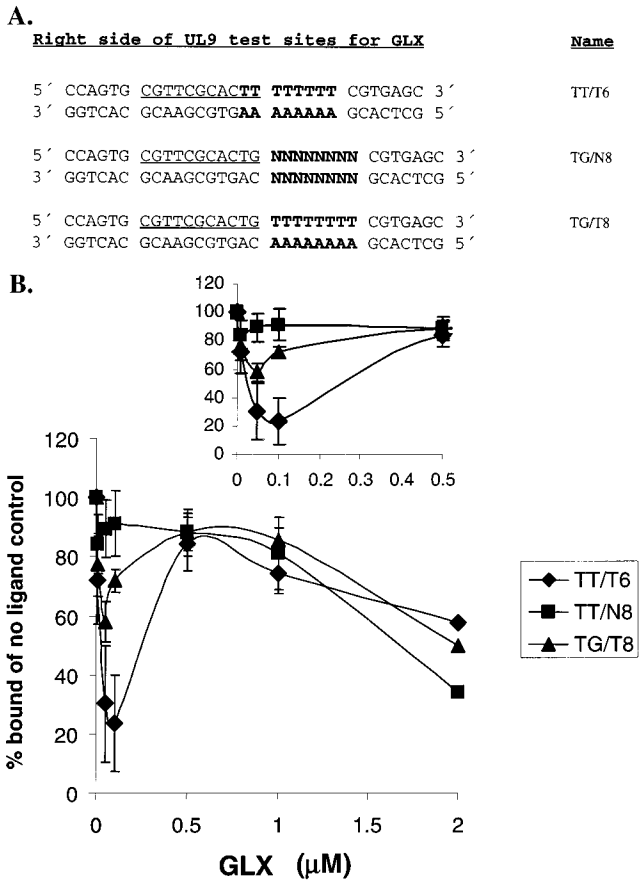

FIGURE 4: Effects of GLX, an indole-linked dimer of netropsin, on UL9 displacement from the right side of the protein. (A) ODNs used in this study. (B) Quantitative analysis, represented by a graph, which was described in Figure 2C. The inset depicts an expanded scale for the low concentration range of ligand.

Interaction of GLX, an Indole-Linked Dimer of Netropsin, on the Right Side of the UL9−DNA Complex. Netropsin and distamycin, which contain two or three pyrrole rings, bind with moderate affinity and to short target sequences of 4−5 bp. To increase the binding affinity and the ability to recognize longer target sequences, an indole-linked dimer of netropsin-like dipyrrole polyamides, GLX (Figure 1), was synthesized. In a separate study, this dimer was determined to bind with greater than 10-fold increased affinity to a minimum of 7−8 bp of AT sequence, compared to netropsin binding to a 4-bp AT site, as indicated by DNase I footprinting and fluorescence HSA results (*29*). The ODNs designed for testing the interaction of GLX with DNA and UL9 (Figure 4A) are similar to those for testing netropsin interactions, except that the engineered ligand binding sites are 8-bp A tracts instead of 4-bp AT sequences, to accommodate the larger binding site size of GLX. When forced to bind at the right side of UL9, in which the ligand binding sites overlap with the protein binding site by 2 bp (ODNs TT/T6 for GLX and TT/TT for netropsin), the IC_{50} value for UL9 displacement for GLX is 20 nM, compared with 0.8 μM for netropsin (Figure 4B). These results clearly demonstrate the benefit of dimerization on the displacement of UL9. In other words, the ability of the linked dimer ligand to displace UL9 is about 40 times better than that of the monomer ligand.

In addition to the enhanced efficacy of UL9 displacement, a concentration-dependent biphasic behavior is observed with

GLX. At 100 nM, GLX achieves maximum protein displacement efficiency with the overlapping ODN TT/T6, but is much less effective as the drug concentration is increased to 500 nM (Figure 4B). This unique biphasic behavior of GLX indicates that there might be two binding modes involved. (1) At low ligand concentration (below 100 nM), it interacts with DNA with one binding mode, effectively disrupting the UL9−DNA complex. (2) At 500 nM concentration, it interacts with DNA with a different binding mode, which has little effect on the protein−DNA complex. With the nonoverlapping ODN TG/T8, much less protein displacement was seen at 50 nM GLX. With control oligonucleotide TG/N8, no significant displacement of UL9 was observed until the concentration of GLX reached 2 μM. At this concentration, GLX probably "coats" the whole length of the DNA nonspecifically, since it shows protein displacement ability that does not discriminate among all three ODNs, TT/T6, TG/T8, and TT/N8, and results in formation of nonsoluble aggregates in the EMSA sample loading wells that do not migrate into the gels.

Interaction of GLX with the Left Side of the UL9−DNA Complex. Our previous studies have suggested that the binding sites of MGBLs, both unitary and dimerized, are required to overlap the right side of the UL9 binding site by about two base pairs in order to achieve maximally effective ligand-induced protein displacement. When the ligand binding sites are placed on the left side of the protein and overlap the UL9 binding site by one base pair, no significant sequence-specific ligand-induced protein displacement is observed (Figure 2D; data for netropsin and GLX not shown). To determine whether an increased overlap on the left side of UL9 can enhance the displacement efficiency by MGBLs, ODNs were designed so as to place the GLX binding site on the left side with additional base-pair overlaps. The right side or both side MGBL binding site(s) containing ODNs also was (were) used in comparison (Figure 5A). In this design, only four Ts were added to the left side, and the first C in the UL9 recognition sequence was changed to a T. Thus, the engineered binding site for GLX on the left side of the protein is TTTTTGTT, which overlaps the protein binding site by four base pairs. By hybridization stabilization and footprinting assays, GLX has been shown to bind to this 8-bp sequence with one GC base pair inserted in the midst of a tract of 7 AT bp (*29*). Using the EMSA, we demonstrated that GLX efficiently displaces UL9 when bound overlapping the right side and both sides of the protein with IC_{50} values of 20 nM (Figure 5B). However, when the ligand binding site is placed overlapping the left side of the protein binding site by four base pairs, no significant displacement is observed until the concentration of GLX reaches 0.5 μM. These results again suggest the presence of a functionally unique ligand binding register on the right side of the UL9 protein binding site. Interestingly, the biphasic displacement curve only was observed with the ODN with the right-side GLX binding site, but was insignificant when the MGBL binding site was placed on both sides of the protein binding site (Figure 5B).

OP_2-Cu Cleavage of the Natural UL9 Site Sequence DNA and Footprinting of the Complex with UL9. The apparent competition between the major groove binding protein UL9 (*19*−*21*) and MGBLs that bind adjacently and overlapping the right side of the UL9 protein binding site suggests the possibility of minor groove distortion by the protein. To test this hypothesis, we employed OP_2-Cu cleavage (*32*, *40*, *41*) on the UL9−DNA complex. In this experiment, the natural UL9 protein binding site (5′-CGTTCGCACTT-3′) that is identical to Box I in the HSV-1 origins of DNA replication was used (Figure 6A). In the presence of UL9, a region of attenuated cleavage by OP_2-Cu that covers the 11-bp UL9 binding site is readily evident (Figure 6). The protection extends from −1 to +3 on the (+) strand and from −2 to +3 on the (−) strand. This result indicates that either UL9 directly blocks easy access of the minor groove or UL9 induces a structural change of the minor groove that attenuates the cleavage by the OP_2-Cu complex in the minor groove.

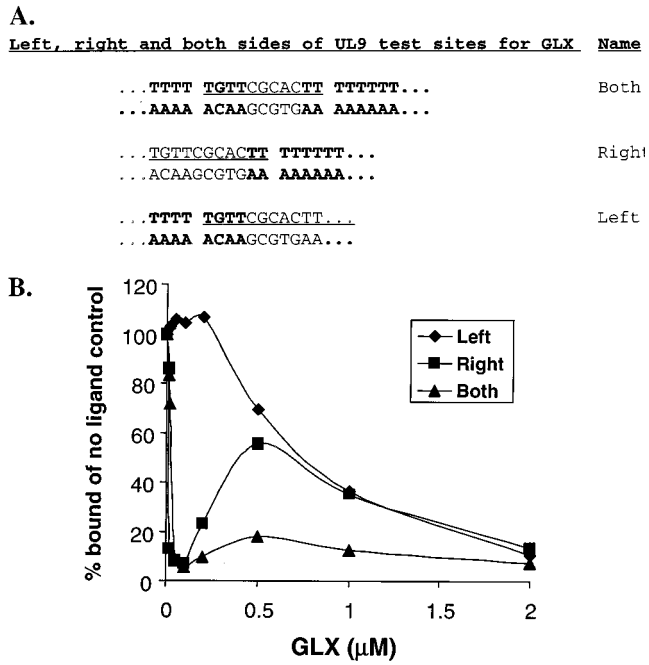

FIGURE 5: Effects of GLX, an indole-linked dimer of netropsin, on UL9 displacement from left side of the protein. (A) ODNs used in this study. (B) Quantitative analysis, represented by a graph, which was described in Figure 2C.

OP_2-Cu Cleavage of the Right Side of UL9 Site A-8 Tract DNA and Footprinting of Complexes with UL9 and with GLX Overlapping the UL9 Site by Two Base Pairs. In the presence of UL9 (lanes 12 and 13, Figure 7A), the cleavage efficiency of OP_2-Cu within the UL9 binding sequence 5′-TGTTCG-CACTT-3′ of the engineered A-8 tract DNA was reduced (Figure 7B), which is in agreement with the result on the nonengineered ODN (Figure 6). Surprisingly, the reactivity of OP_2-Cu on the flanking A-8 tract was significantly enhanced in the presence of UL9, which was not seen with the nonengineered ODN. This result indicates that the minor groove of the adjacent, overlapping A-tract region was opened up upon UL9 binding, rendering it more accessible to the cleavage agent. In contrast, the cleavage by OP_2-Cu of the A-tract region was inhibited in the presence of GLX (lanes 4−11, Figure 7A). At low concentrations of GLX (31 nM), the protection extends to +3 on the A-tract of the (+) strand and to −2 of the (−) strand with 5′-to-3′ offset, an indication of minor groove interaction of this ligand (Figure 7B). At this concentration, GLX showed good protein displacement ability in the EMSA. In addition, the region footprinted by GLX at this concentration was limited to 10

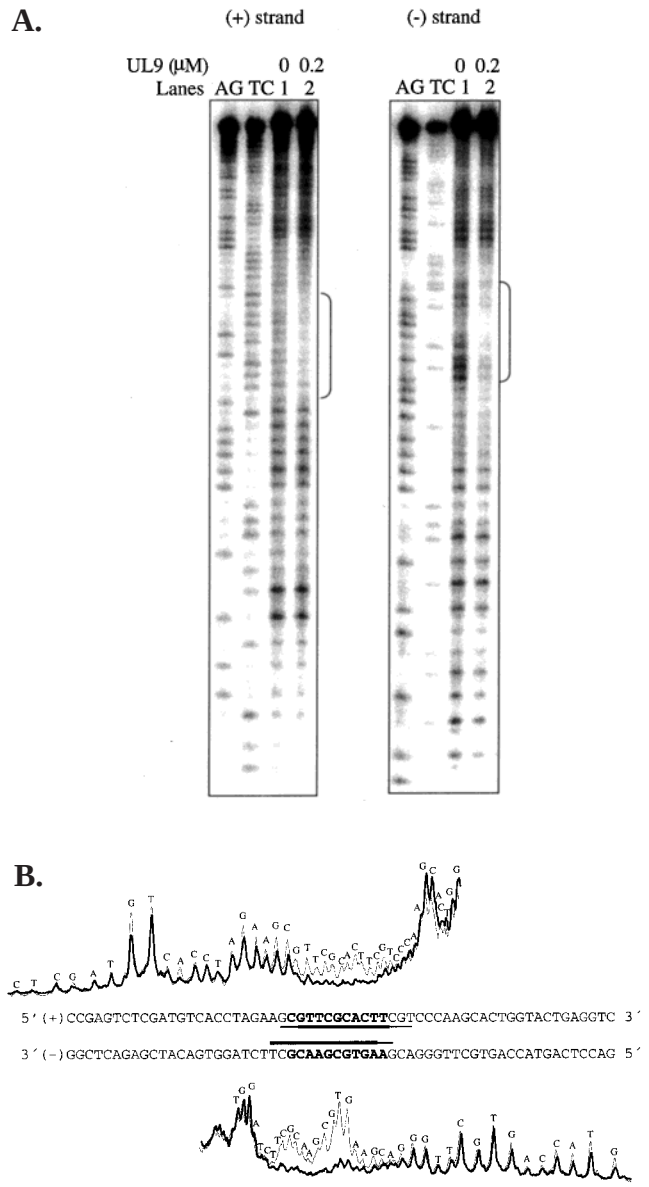

FIGURE 6: OP_2-Cu footprints of the UL9−DNA complex. (A) Autoradiogram of a 12% denaturing polyacrylamide gel showing the OP_2-Cu cleavage pattern in the absence (lane 1) and in the presence (lane 2) of UL9. Lanes AG and TC contain the Maxam−Gilbert sequencing reactions (*46*). Lanes 1 and 2 contain 0 and 0.2 μM UL9 protein. (B) PhosphorImager scans of lanes 1 and 2 and a diagram illustrating the sequences protected by UL9. The thin and thick lines of the scans represent lanes 1 and 2, respectively. In the diagram, thick and thin straight lines opposing specific sequence positions represent strong and weak footprint regions, respectively.

bp, suggesting the ligand binds in a 1:1 mode to the A-tract (Figure 7B). However, at higher concentrations of GLX (500 nM), which showed weak protein displacement ability in the EMSA, the region of footprint extended beyond the A-tract (Figure 7B), indicating an extended binding site of GLX.

Binding Stoichiometry between GLX and the A-8 Tract DNA. At higher concentrations, an enlarged footprint region was seen with GLX. This extended binding mode could be a result of a staggered side-by-side 2:1 binding mode of GLX. To study the binding mode of GLX to the A-8 tract region, an 11-bp DNA ODN, 5′-CGAAAAAAAAG-3′ (FQ11), was designed (Figure 8). The HSA, monitored using fluorescence spectroscopy, was used as described under Experimental Procedures to study the binding stoichiometry. Figure 8 shows the fluorescence change in a continuous variation experiment. The molar fraction of the ligand was varied from 0 to 1, with the total concentration of DNA (FQ11) and ligand kept constant at 0.5 μM. The rising and declining regions of the titration can be fitted by linear regression. The intersection of the two lines yields a GLX molar fraction of 0.68 ± 0.09, indicating the preferred binding sequence, single site specific GLX:DNA ratio is 2:1. Because a single GLX molecule occupies approximately 8 bp, FQ11 DNA is too short for two GLX to bind in a linear tandem orientation, which would have to encompass the unfavorable distal GC base pairs and would overlap the ends of the DNA complex.

DISCUSSION

Steric Inhibition of Protein Binding by MGBLs. It has been known for a long time that MGBLs can block the binding of minor groove binding proteins, such as TBP (*6*), or other proteins whose contacts in the minor groove are critical for protein−DNA binding affinity, such as TFIIIA (*7, 12*). The binding inhibition is thought to be the consequence of direct steric competition between the MGBLs and the proteins for a common site(s) within the DNA minor groove. However, other proteins, including the majority of transcription factors, contact DNA primarily, or solely, through contacts with the major groove, which presents a challenge to the use of sequence-specific MGBLs to disrupt the binding of these major groove interacting proteins. One successful approach has been to attach a positively charged polyamine or polypeptide patch to the synthetic polyamide MGBLs. These chemical additions both neutralize the charges of the DNA backbone, so as to interfere with major groove interacting proteins contacting through the phosphates, and sterically block access of the proteins to the major groove (*11, 14*).

Allosteric Inhibition by MGBLs Binding on the Right Side of UL9. In the present model study of a purely major groove binding protein, for which the structure of the complex with DNA has not been determined, we have avoided additional chemical modifications of MGBLs by identifying allosteric interactions on the right side of the UL9 protein recognition sequence. In a previous study, Simonsson and co-workers determined that the distal two TT on the right side of the UL9 binding site were not contacted by the protein through the major groove (*28*). Our own investigation using a PCR-based selection assay also showed that the first and last base positions within the 11-bp recognition site 5′-CGTTCG-CACTT-3′ are the least conserved positions (unpublished results), indicating UL9 might not have direct contacts with these base pairs. Here we demonstrated that MGBLs such as distamycin, netropsin, and an indole-linked dimer of netropsin-like di-pyrroles, GLX, effectively displace UL9 only with the ODNs whose engineered ligand binding sites overlap with the last two TT on the right side of the protein binding site. There are two possible explanations for these observations. (1) UL9 may contact these TT bases through the minor groove, and, consequently, the displacement observed is a result of direct steric competition between the protein and these MGBLs at the same sites. (2) UL9 may induce a DNA conformational change at the right side of its binding site, including the last two TT bases, and the protein displacements arise from allosteric inhibitions. As sum-

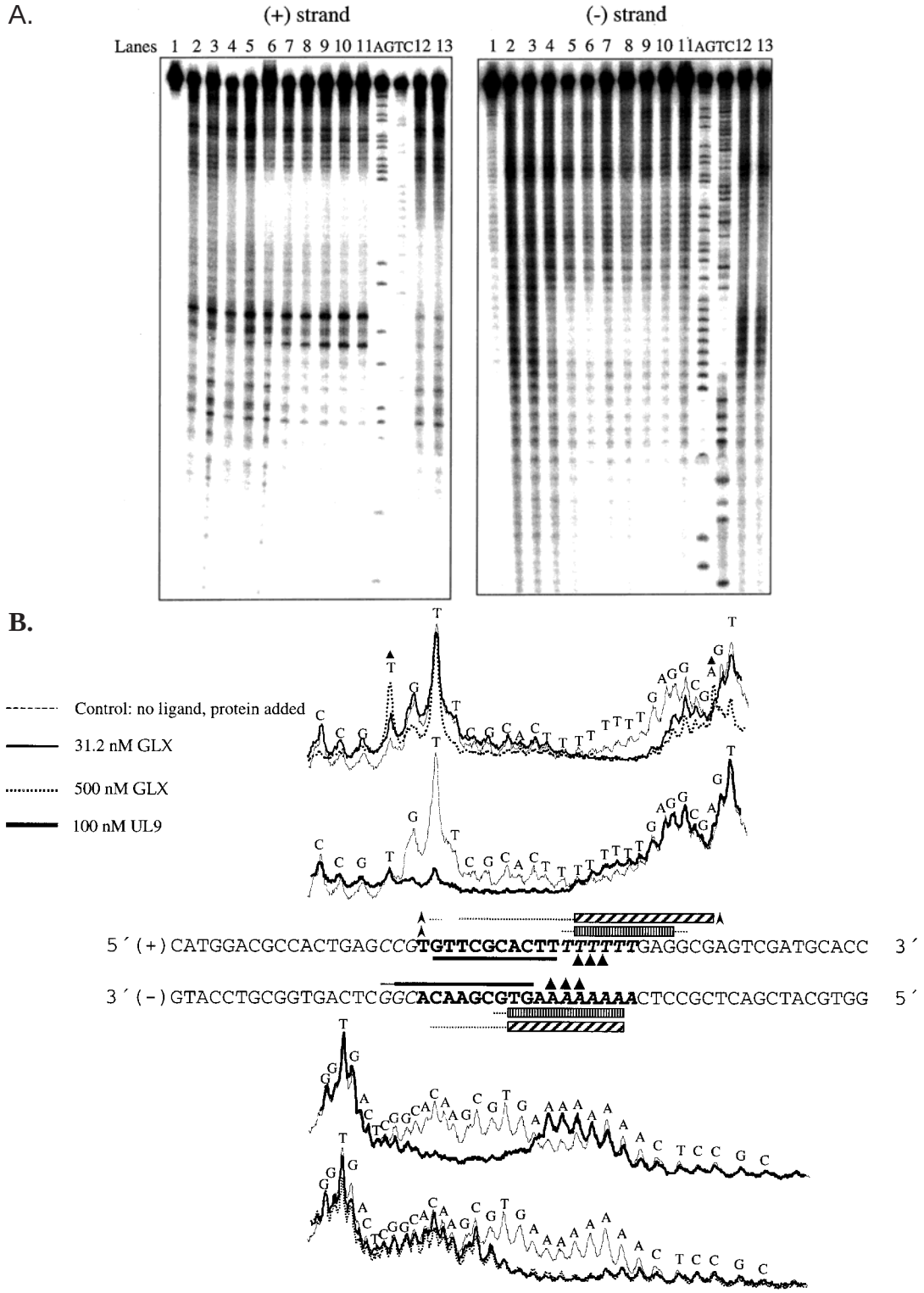

FIGURE 7: OP_2-Cu footprint of UL9−DNA and GLX−DNA complexes on the right side overlapping ODN. (A) Autoradiogram of a 12% denaturing polyacrylamide gel showing the footprints in the presence of UL9 or GLX. Lanes AG and TC contain the Maxam−Gilbert sequencing reactions. Lane 1 contains DNA without any treatment. Lanes 2−11 contain 0, 0, 7.8, 15.6, 31.2, 62.5, 125, 250, 500, and 1000 nM GLX, respectively. Lanes 12 and 13 contain 100 nM UL9. (B) PhosphorImager scans and a diagram illustrating the OP_2-Cu cleavage patterns. In the diagram, thick and thin straight lines parallel to the ODN sequences represent strong and weak footprint regions, respectively, in the presence of UL9. The big solid arrows indicate the enhanced OP_2-Cu cleavage sites in the presence of the protein. The rectangular box with vertical bars and the adjacent dotted line indicate the strong and weak footprint regions at 31 nM GLX, respectively. The rectangular box with diagonal bars and the adjacent dotted line indicate the strong and weak footprint regions at 500 nM GLX, respectively. The small arrows represent the enhanced OP_2-Cu cleavage sites in the presence of the ligand.

marized earlier, there is no direct evidence supporting explanation (1). In the presence of the protein, the yield of OP_2-Cu cleavage products in the central part of the UL9 recognition site was diminished, while the cleavage at the flanking right side A-tract region was enhanced, especially at the second A of the bottom strand (Figure 7B). These

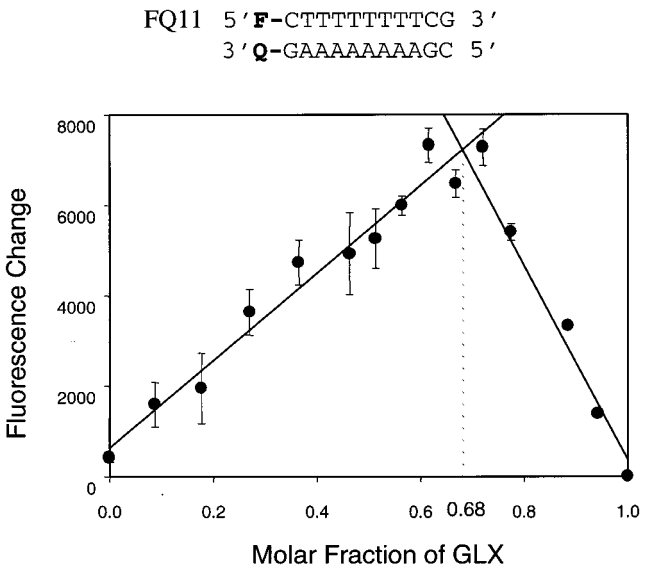

FIGURE 8: Continuous variation assay to determine the binding stoichiometry of GLX to the 11-bp ODN containing an A-8 tract (FQ11). The total concentration of GLX and FQ11 was kept constant at 0.5 μM. The changes in fluorescence due to ligand binding were monitored as a function of the molar fraction of GLX. Linear regressions were performed, and the intercept of the two best-fitted lines is 0.68 $\pm$ 0.09, indicating a 2:1 binding stoichiometry. The error bars represent standard deviations obtained from the duplicate experiments.

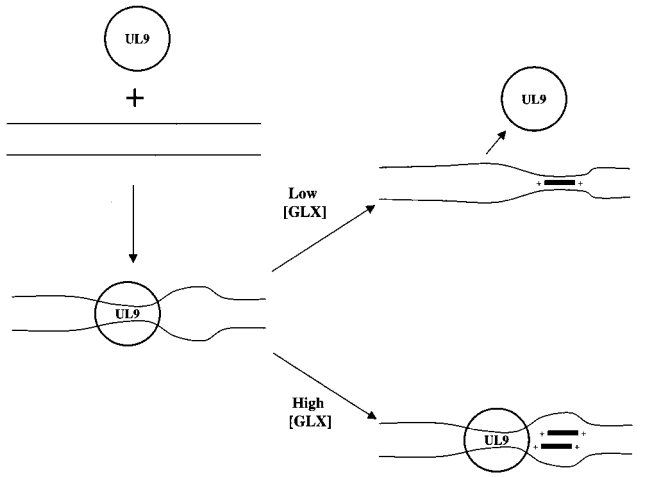

FIGURE 9: Schematic representation of ligand binding stoichiometry dependent allosteric destabilization of UL9−DNA complexes by GLX.

results suggest that binding of UL9 to the major groove narrows the opposing minor groove of the core recognition region by local bending and/or overwinding. Simultaneously, a minor groove widening conformational change is induced at the flanking A-tract, including the last two TT bases (Figure 9), consistent with local DNA relaxation. These findings make the first suggestion even less likely, since the protein would have blocked OP_2-Cu cleavage if it had contacted these last two TT bases through the minor groove. Therefore, we favor the explanation that a DNA conformational change, rather than a direct steric impediment by the ligands at the protein binding site, accounts for the UL9 displacement caused by binding of these MGBLs at engineered A-tracts overlapping the right side of the protein binding sequence by 2 bp.

Effective UL9 displacement occurred when the binding sites of these MGBLs were placed on the right side of the protein. However, no significant displacement was detected until the drug concentrations were much higher when ligand binding sites were engineered on the left side of the protein with one or four base-pair overlaps. These observations suggested asymmetric contacts of UL9 with the left and right sides of DNA sequences. Although UL9 binds to DNA as a homodimer, it has been shown recently by cross-linking that only one of the two monomers contacts DNA (*25*). Elsewhere, asymmetric DNA binding for homodimeric basic helix−loop−helix transcription factors and subsequent asymmetric displacement by MGBLs have been observed (*42*). In addition, the DNA conformational change induced upon UL9 binding was only observed on the right side of the protein, which agrees with the protein displacement studies, indicating the requirement for a unique ligand binding register on the right side of the protein. The extent of protein displacement induced by GLX depends on the engineered DNA sequences as well as the compound concentration. No significant differences in UL9−DNA binding were observed for all of the sequences tested including the A-tract, consistent with published data (*24*) that demonstrated that only the central 9-bp sequence 5′-GTTCGCACT-3′ within the UL9 binding site is conserved. Although the A-tract has a narrower groove that may be less favorable for the initial binding of UL9, the overall binding affinity was not affected, presumably because the flanking A-tract is also thermodynamically more easily melted and distorted than the natural sequence. For optimal sequences, approximately 95% of the UL9−DNA complex was dissociated at 20 nM GLX (cf. Figure 5B). For some sequences, maximum protein displacement was difficult to quantify due to the formation of nonsoluble aggregates in the EMSA sample loading wells that did not migrate into the gels. However, there is good reason to suspect that somewhat less than 100% effective disruption of UL9−DNA complexes, and, by inference, of transcription factor−DNA complexes in general, may be all that is required for effective regulation of gene expression. For example, antisense data from multiple studies suggest that only a 3−4-fold down-regulation of cyclin D1, equivalent to 66−75% inhibition of transcription factor binding to a key critical regulatory element, is sufficient to impact the disease state in breast cancer (see *29*).

Multiple Binding Modes of GLX. The concentration-dependent biphasic behavior of GLX in UL9 displacement indicates there might be multiple binding modes involved. This biphasic behavior is not unique to UL9 since it has been observed for interactions of GLX with other proteins, such as LEF-1 (unpublished data), implying it is a property of the ligand instead of the protein. GLX can effectively displace UL9 at low ligand concentrations, such as 20 nM. At this concentration, GLX may bind to the A-8 tract in a 1:1 mode, which requires a relatively narrow minor groove (Figure 9). The narrow minor groove required for DNA binding by the ligand at this lower concentration is incompatible with the wider A-8 minor groove that UL9 produces upon binding; consequently, the binding of the ligand to the A-tract disrupts the UL9−DNA complex via inducing a DNA conformational change. At high ligand concentrations, GLX could bind to the A-tract as a 2:1 ring-stacked mode, which needs a wider minor groove in which to bind. Since UL9

widens the minor groove of the A-tract at the right side, 2:1 GLX binding to the A-tract region and adjacent UL9 binding can be co-accommodated (Figure 9). This could explain why less protein displacement was observed at higher ligand concentrations. One should note that other types of DNA conformational changes, such as DNA local unwinding and bending, can result in a widened minor groove and may be important to the biphasic displacement behavior. The essence of the proposed model (illustrated in Figure 9) lies in that DNA conformational changes induced by GLX in the 1:1 bound state and by the GLX dimer are *distinct* in that the 2:1 bound DNA is conformationally compatible with the binding of UL9.

We observed a diminished biphasic behavior when ligand binding sites were engineered on both sides of the UL9 site (cf. Figure 5B). The displacement curve is approximately a result of the combined effect when the GLX binding site was only on either the left or the right side of the UL9 site. For example, at 0.5 μM GLX, where the biphasic behavior is most dramatic, UL9 displacements were 30% and 55%, respectively, when ligand binding sites were placed on either the left or the right side alone. If one assumes the two ligand binding sites are independent, the combined effect should be approximately 69%[2] displacement based on the two individual contributions, close to the observed displacement for ODNs with ligand binding sites on both sides of the UL9 site (~82%). This observation is consistent with an additive effect from independent contributions when the ligand binding site was placed on the left side or the right side of the UL9 binding site.

Our quantitative HSA binding studies showed that the binding stoichiometry between GLX and the 11-bp ODN 5′-CGAAAAAAAAG-3′ is 2:1 at elevated concentrations (Figure 8). This 11-bp ODN is too short for GLX to bind end-to-end as tandem monomers without overhanging the ends of the duplex and forfeiting significant potential binding energy. A greater realization of surface complementary binding interaction is more likely if this rigidly extended conformation, coplanar MGBL binds in a side-by-side ring-stacked mode. A ring-stacked 2:1 binding stoichiometry has been observed previously for a number of DNA binding ligands. It has been shown that monocationic distamycin binds to DNA in a 2:1 mode, where two distamycin molecules stack in an antiparallel fashion (*39*). The 2:1 binding mode will result in a widened minor groove, as indicated by NMR measurements. However, we did not observe a biphasic displacement with the flanking TA/ATT sequence for distamycin, even though it has been shown that distamycin dimerizes in the minor groove of a 5-bp AT stretch (*39*). This monotonic displacement for distamycin is likely caused by several factors relating to different flanking sequences, ligand binding site sizes, and distamycin binding cooperativity. The UL9 flanking region TA/ATT sequence for distamycin is different from TT/T6 (an 8-bp A-tract) for GLX. Whereas UL9 binding enhanced the OP_2-Cu cleavages on the flanking A-tract (Figure 7), no enhancement was seen on the flanking region of the natural sequence without the A-tract (Figure 6), indicating that the presence of an A-tract might facilitate structural distortion by UL9, thus promoting the allosteric inhibitions of UL9 binding by GLX. The binding site size for distamycin is about half of that for GLX, which means the nonspecific binding of distamycin is more pronounced than GLX. Because distamycin displaces UL9 at much higher concentrations, nonspecific binding may interfere with any potential biphasic displacement. Since binding of distamycin to a number of five consecutive AT base pairs, similar to TA/ATT, has been shown to be cooperative (*38*), a potential cooperative binding of distamycin to TA/ATT also may lead to the monophasic displacement of UL9.

Although netropsin, a dicationic ligand, was found to bind only in a 1:1 mode (*43*, *44*), possibly due to the repulsion of the two positive charges at both ends, a recent study demonstrated that other dicationic ligands can bind to DNA in a stacked 2:1 mode (*45*). Due to the two positive charges, one at either end, it is probable that GLX binds DNA in a staggered orientation, where the two molecules overlap only partially. Consistent with this interpretation, the OP_2-Cu footprinting results showed an extended region of protection from cleavage at the elevated concentrations of GLX determined to give 2:1 binding, compared to lower concentrations. Further studies of the interaction of GLX with DNA will be published separately (Zhang et al., submitted for publication).

Applications in Gene Regulation. The abilities of sequence-specific MGBLs to allosterically displace DNA major groove binding proteins present opportunities for the use of these small molecules in gene regulation. One example is to use GLX in a gene switch system which utilizes a chimeric transactivator composed of a fusion of UL9, as the DNA binding domain, and VP-16, as the transactivation domain (unpublished data). In this system, when the binding sites of this chimeric transactivator are flanked by the binding sites of GLX, the binding of the transactivator can be controlled by the ligand; i.e., bound transactivator can be allosterically displaced by the ligand from a promoter that contains a response element consisting of appropriately overlapping ligand binding and factor binding sequences. The displacement of the transactivator leads to the down-regulation of the transcription of the transgene (switch-off by effector ligand). Our latest results suggest that GLX can down-regulate a reporter gene in a transient transfection cell-based assay (unpublished data). The GLX−DNA binding stoichiometry dependent biphasic disruption of UL9−DNA binding also suggests the opportunity to engineer gene switch systems with more precise control over a defined effector ligand concentration range. Most importantly, while it should not be expected that allosteric facilitation of displacement of major groove DNA binding regulatory proteins by MGBLs will be a universal mechanism, it can be expected that other examples will be found. In such cases, to disrupt protein−DNA complexes and control gene expression, it may prove most economically effective to leverage allosteric interactions of minimally designed MGBLs.

[2] The combined displacement of UL9 was estimated as (55% + 30%) − 55% × 30% = 69%. The subtraction is necessary because the site doubly occupied by GLX would only displace one UL9 but was counted twice. This estimation is valid only when the binding events to the left and right sides are independent and GLX is in excess of its binding sites.

ACKNOWLEDGMENT

We thank Dr. Cynthia Edwards for introduction to the problem of MGBL interactions with UL9−DNA complexes

and for early discussions, Lisa Turin for some independently performed confirmatory studies, John Deikman for unpublished results with LEF-1 protein, and Dr. Moon Lim for unpublished results using UL9 fusion proteins as gene switches.

REFERENCES

1. Wemmer, D. E. (2000) *Annu. Rev. Biophys. Biomol. Struct. 29*, 439−461.
2. Berg, J. M., and Godwin, H. A. (1997) *Annu. Rev. Biophys. Biomol. Struct. 26*, 357−371.
3. Pabo, C. O., Peisach, E., and Grant, R. A. (2001) *Annu. Rev. Biochem. 70*, 313−340.
4. Wemmer, D. E., and Dervan, P. B. (1997) *Curr. Opin. Struct. Biol. 7*, 355−361.
5. Reddy, B. S., Sondhi, S. M., and Lown, J. W. (1999) *Pharmacol. Ther. 84*, 1−111.
6. Chiang, S. Y., Welch, J., Rauscher, F. J., III, and Beerman, T. A. (1994) *Biochemistry 33*, 7033−7040.
7. Gottesfeld, J. M., Neely, L., Trauger, J. W., Baird, E. E., and Dervan, P. B. (1997) *Nature 387*, 202−205.
8. Clemens, K. R., Liao, X., Wolf, V., Wright, P. E., and Gottesfeld, J. M. (1992) *Proc. Natl. Acad. Sci. U.S.A. 89*, 10822−10826.
9. Clemens, K. R., Zhang, P., Liao, X., McBryant, S. J., Wright, P. E., and Gottesfeld, J. M. (1994) *J. Mol. Biol. 244*, 23−35.
10. Hayes, J. J., and Tullius, T. D. (1992) *J. Mol. Biol. 227*, 407−417.
11. Chiang, S. Y., Bruice, T. C., Azizkhan, J. C., Gawron, L., and Beerman, T. A. (1997) *Proc. Natl. Acad. Sci. U.S.A. 94*, 2811−2816.
12. Neely, L., Trauger, J. W., Baird, E. E., Dervan, P. B., and Gottesfeld, J. M. (1997) *J. Mol. Biol. 274*, 439−445.
13. Oakley, M. G., Mrksich, M., and Dervan, P. B. (1992) *Biochemistry 31*, 10969−10975.
14. Bremer, R. E., Baird, E. E., and Dervan, P. B. (1998) *Chem. Biol. 5*, 119−133.
15. Love, J. J., Li, X., Case, D. A., Giese, K., Grosschedl, R., and Wright, P. E. (1995) *Nature 376*, 791−795.
16. Dickinson, L. A., Gulizia, R. J., Trauger, J. W., Baird, E. E., Mosier, D. E., Gottesfeld, J. M., and Dervan, P. B. (1998) *Proc. Natl. Acad. Sci. U.S.A. 95*, 12890−12895.
17. Dorn, A., Affolter, M., Muller, M., Gehring, W. J., and Leupin, W. (1992) *EMBO J. 11*, 279−286.
18. Olivo, P. D., Nelson, N. J., and Challberg, M. D. (1988) *Proc. Natl. Acad. Sci. U.S.A. 85*, 5414−5418.
19. Elias, P., O'Donnell, M. E., Mocarski, E. S., and Lehman, I. R. (1986) *Proc. Natl. Acad. Sci. U.S.A. 83*, 6322−6326.
20. Bruckner, R. C., Crute, J. J., Dodson, M. S., and Lehman, I. R. (1991) *J. Biol. Chem. 266*, 2669−2674.
21. Fierer, D. S., and Challberg, M. D. (1992) *J. Virol. 66*, 3986−3995.
22. Weir, H. M., Calder, J. M., and Stow, N. D. (1989) *Nucleic Acids Res. 17*, 1409−1425.
23. Elias, P., Gustafsson, C. M., and Hammarsten, O. (1990) *J. Biol. Chem. 265*, 17167−17173.
24. Hazuda, D. J., Perry, H. C., Naylor, A. M., and McClements, W. L. (1991) *J. Biol. Chem. 266*, 24621−24626.
25. Lee, S. S., and Lehman, I. R. (1999) *J. Biol. Chem. 274*, 18613−18617.
26. Fierer, D. S., and Challberg, M. D. (1995) *J. Biol. Chem. 270*, 7330−7334.
27. Koff, A., and Tegtmeyer, P. (1988) *J. Virol. 62*, 4096−4103.
28. Simonsson, S., Samuelsson, T., and Elias, P. (1998) *J. Biol. Chem. 273*, 24633−24639.
29. Laurance, M. E., Starr, D. B., Michelotti, E. F., Cheung, E., Gonzalez, C., Tam, A. W., Deikman, J., Edwards, C. A., and Bardwell, A. J. (2001) *Nucleic Acids Res. 29*, 652−661.
30. Fishleigh, R. V., Fox, K. R., Khalaf, A. I., Pitt, A. R., Scobie, M., Suckling, C. J., Urwin, J., Waigh, R. D., and Young, S. C. (2000) *J. Med. Chem. 43*, 3257−3266.
31. Martinez, R., and Edwards, C. A. (1993) *Protein Expression Purif. 4*, 32−37.
32. Sigman, D. S., Kuwabara, M. D., Chen, C. H., and Bruice, T. W. (1991) *Methods Enzymol. 208*, 414−433.
33. Job, P. (1928) *Ann. Chim. (Paris) 9*, 113−203.
34. Pelton, J. G., and Wemmer, D. E. (1988) *Biochemistry 27*, 8088−8096.
35. Portugal, J., and Waring, M. J. (1987) *FEBS Lett. 225*, 195−200.
36. Abu-Daya, A., Brown, P. M., and Fox, K. R. (1995) *Nucleic Acids Res. 23*, 3385−3392.
37. Van Dyke, M. W., Hertzberg, R. P., and Dervan, P. B. (1982) *Proc. Natl. Acad. Sci. U.S.A. 79*, 5470−5474.
38. Chen, F. M., and Sha, F. (1998) *Biochemistry 37*, 11143−11151.
39. Pelton, J. G., and Wemmer, D. E. (1989) *Proc. Natl. Acad. Sci. U.S.A. 86*, 5723−5727.
40. Papavassiliou, A. G. (1995) *Biochem. J. 305 (Pt. 2)*, 345−357.
41. Spassky, A., and Sigman, D. S. (1985) *Biochemistry 24*, 8050−8056.
42. Winston, R. L., Ehley, J. A., Baird, E. E., Dervan, P. B., and Gottesfeld, J. M. (2000) *Biochemistry 39*, 9092−9098.
43. Kopka, M. L., Yoon, C., Goodsell, D., Pjura, P., and Dickerson, R. E. (1985) *Proc. Natl. Acad. Sci. U.S.A. 82*, 1376−1380.
44. Chen, X., Mitra, S. N., Rao, S. T., Sekar, K., and Sundaralingam, M. (1998) *Nucleic Acids Res. 26*, 5464−5471.
45. Wang, L., Bailly, C., Kumar, A., Ding, D., Bajic, M., Boykin, D. W., and Wilson, W. D. (2000) *Proc. Natl. Acad. Sci. U.S.A. 97*, 12−16.
46. Maxam, A. M., and Gilbert, W. (1980) *Methods Enzymol. 65*, 499−560.

BI0109865